

University of Groningen

## MYD88 mutations identify a molecular subgroup of diffuse large B-cell lymphoma with an unfavorable prognosis

Vermaat, Joost S.; Somers, Sebastiaan F.; de Wreede, Liesbeth C.; Kraan, Willem; de Groen, Ruben A. L.; Schrader, Anne M. R.; Kerver, Emile D.; Scheepstra, Cornelis G.; Berenschot, Henriette; Deenik, Wendy

*Published in:*  
Haematologica

*DOI:*  
[10.3324/haematol.2018.214122](https://doi.org/10.3324/haematol.2018.214122)

**IMPORTANT NOTE: You are advised to consult the publisher's version (publisher's PDF) if you wish to cite from it. Please check the document version below.**

*Document Version*  
Publisher's PDF, also known as Version of record

*Publication date:*  
2020

[Link to publication in University of Groningen/UMCG research database](#)

### *Citation for published version (APA):*

Vermaat, J. S., Somers, S. F., de Wreede, L. C., Kraan, W., de Groen, R. A. L., Schrader, A. M. R., Kerver, E. D., Scheepstra, C. G., Berenschot, H., Deenik, W., Wegman, J., Broers, R., De Boer, J-P. D., Nijland, M., van Wezel, T., Veelken, H., Spaargaren, M., Cleven, A. H., Kersten, M. J., & Pals, S. T. (2020). MYD88 mutations identify a molecular subgroup of diffuse large B-cell lymphoma with an unfavorable prognosis. *Haematologica*, 105(2), 424-434. <https://doi.org/10.3324/haematol.2018.214122>

### **Copyright**

Other than for strictly personal use, it is not permitted to download or to forward/distribute the text or part of it without the consent of the author(s) and/or copyright holder(s), unless the work is under an open content license (like Creative Commons).

The publication may also be distributed here under the terms of Article 25fa of the Dutch Copyright Act, indicated by the "Taverne" license. More information can be found on the University of Groningen website: <https://www.rug.nl/library/open-access/self-archiving-pure/taverne-amendment>.

### **Take-down policy**

If you believe that this document breaches copyright please contact us providing details, and we will remove access to the work immediately and investigate your claim.



Journal of The Ferrata Storti Foundation

## MYD88 mutations identify a molecular subgroup of diffuse large B-cell lymphoma with an unfavourable prognosis

by Joost S. Vermaat, Sebastiaan F. Somers, Liesbeth C. de Wreede, Willem Kraan, Ruben A.L. de Groen, Anne M.R. Schrader, Emile D. Kerver, Cornelis G. Scheepstra, Henriëtte Beerenschot, Wendy Deenik, Jurgen Wegman, Rianne Broers, Jan-Paul D. de Boer, Marcel Nijland, Tom van Wezel, Hendrik Veelken, Marcel Spaargaren, Arjen H. Cleven, Marie José Kersten, and Steven T. Pals

Haematologica 2019 [Epub ahead of print]

*Citation: Joost S. Vermaat, Sebastiaan F. Somers, Liesbeth C. de Wreede, Willem Kraan, Ruben A.L. de Groen, Anne M.R. Schrader, Emile D. Kerver, Cornelis G. Scheepstra, Henriëtte Beerenschot, Wendy Deenik, Jurgen Wegman, Rianne Broers, Jan-Paul D. de Boer, Marcel Nijland, Tom van Wezel, Hendrik Veelken, Marcel Spaargaren, Arjen H. Cleven, Marie José Kersten, and Steven T. Pals. MYD88 mutations identify a molecular subgroup of diffuse large B-cell lymphoma with an unfavourable prognosis.*

*Haematologica. 2019; 104:xxx*

*doi:10.3324/haematol.2018.214122*

### *Publisher's Disclaimer.*

*E-publishing ahead of print is increasingly important for the rapid dissemination of science. Haematologica is, therefore, E-publishing PDF files of an early version of manuscripts that have completed a regular peer review and have been accepted for publication. E-publishing of this PDF file has been approved by the authors. After having E-published Ahead of Print, manuscripts will then undergo technical and English editing, typesetting, proof correction and be presented for the authors' final approval; the final version of the manuscript will then appear in print on a regular issue of the journal. All legal disclaimers that apply to the journal also pertain to this production process.*

# **MYD88 mutations identify a molecular subgroup of diffuse large B-cell lymphoma with an unfavourable prognosis**

Joost S. Vermaat<sup>1,2,3</sup>, Sebastiaan F. Somers<sup>3</sup>, Liesbeth C. de Wreede<sup>4</sup>, Willem Kraan<sup>2,5</sup>, Ruben A.L. de Groen<sup>3</sup>, Anne M. R. Schrader<sup>6</sup>, Emile D. Kerver<sup>7</sup>, Cornelis G. Scheepstra<sup>8</sup>, Henriëtte Berenschot<sup>9</sup>, Wendy Deenik<sup>10</sup>, Jurgen Wegman<sup>1,11</sup>, Rianne Broers<sup>12</sup>, Jan-Paul D. de Boer<sup>13</sup>, Marcel Nijland<sup>14</sup>, Tom van Wezel<sup>6</sup>, Hendrik Veelken<sup>3</sup>, Marcel Spaargaren<sup>2,5</sup>, Arjen H. Cleven<sup>6</sup>, Marie José Kersten<sup>1,2</sup>, and Steven T. Pals<sup>2,5</sup>

<sup>1</sup>Department of Hematology, Amsterdam University Medical Center, University of Amsterdam, The Netherlands

<sup>2</sup>Lymphoma and Myeloma Center Amsterdam-LYMMCARE, and Cancer Center Amsterdam (CCA) Amsterdam, The Netherlands

<sup>3</sup>Department of Hematology, Leiden University Medical Center, Leiden, The Netherlands

<sup>4</sup>Department of Biomedical Data Sciences, Leiden University Medical Center, Leiden, The Netherlands

<sup>5</sup>Department of Pathology, Amsterdam University Medical Center, University of Amsterdam, The Netherlands

<sup>6</sup>Department of Pathology, Leiden University Medical Center, Leiden, The Netherlands

<sup>7</sup>Department of Internal Medicine & Hematology, Onze Lieve Vrouwe Gasthuis, Amsterdam, The Netherlands

<sup>8</sup>Department of Pathology, Onze Lieve Vrouwe Gasthuis, Amsterdam, The Netherlands

<sup>9</sup>Department of Internal Medicine & Hematology, Albert Schweitzer Hospital, Dordrecht, The Netherlands

<sup>10</sup>Department of Internal Medicine & Hematology, Tergooi Hospital, Hilversum, The Netherlands

<sup>11</sup>Department of Internal Medicine & Hematology, Deventer Hospital, Deventer, The Netherlands

<sup>12</sup>Department of Internal Medicine & Hematology, Waterland Hospital, Purmerend, The Netherlands

<sup>13</sup>Department of Medical Oncology & Hematology, Antoni van Leeuwenhoekziekenhuis, Amsterdam, The Netherlands

<sup>14</sup>Department of Hematology, University Medical Center Groningen, Groningen, The Netherlands

## **Running heads**

*MYD88* mutational status improves classification and prognostication in DLBCL

## **Key words**

*MYD88*, mutational status, classification, prognostication, DLBCL

## **Correspondence**

Joost S.P. Vermaat MD PhD MSc,

Department of Hematology, Leiden University Medical Center, PO Box 9600, 2300 RC Leiden, The Netherlands

E-mail: [j.s.p.vermaat@lumc.nl](mailto:j.s.p.vermaat@lumc.nl)

**Original article**

Number of words in abstract: **276**

Number of words in main text: **4151**

Number of references: **51**

Number of figures/tables: **4 tables and 3 figures,**

Supplemental: **methods, 1 supplemental table and 1 supplemental figure**

**Acknowledgements:**

The authors would like to thank other involved research technicians, data managers and physicians for their contributions to this manuscript.

**Funding resources:**

This study was supported in part by research funding from 'Egbers Stichting AMC Foundation', 'Stichting Fonds Oncologie Holland', and Lymph&Co (J.S.V., S.F.S., R.A.G., A.H.C., W.K., M.S., M.J.K., and S.T.P.).

**Conflicts of interest:**

M.J.K. and M.N. have received honoraria/research funding from Kite Pharma, Millennium/Takeda, Mundipharma, Gilead Sciences, Bristol-Myers Squibb, Roche, Celgene, Novartis Pharmaceuticals Corporation, Merck Sharp & Dohme, and Amgen. M.S. received research funding from Pharmacyclics and Johnson&Johnson.

The other authors do not have any conflicts of interests or disclosure to declare: J.S.V., S.F.S., L.C.W., W.K., R.A.G., A.M.S., E.D.K., H.B., W.D., J.W., R.B., J.D.B., M.N., T.W., H.V., A.H.C, and S.T.P.

**Authorship contribution:**

J.S.V., S.F.S., L.C.W., R.A.G., A.M.S., H.V., M.S., A.H.C., M.J.K., and S.T.P. contributed to the design of the research;

J.S.V., W.K., E.D.K., H.B., W.D., J.W., R.B., J.D.B., M.N., H.V., A.H.C., M.J.K., and S.T.P. contributed to the collection of patient material;

J.S.V., S.F.S., W.K., L.C.W., R.A.G., A.M.S., E.D.K., H.B., W.D., J.W., R.B., J.P.B., M.N., T.W., H.V., M.S., A.H.C., M.J.K., and S.T.P., contributed to the analysis of the data; and

J.S.V., S.F.S., L.C.W., R.A.G., A.M.S., M.N., T.W., H.V., A.H.C., M.J.K., and S.T.P. contributed to the writing of the manuscript.

## **Abstract**

The 2016 WHO classification defines diffuse large B-cell lymphoma subtypes based on EBV infection and oncogenic rearrangements of *MYC/BCL2/BCL6* as drivers of lymphomagenesis. A subset of diffuse large B-cell lymphoma, however, is characterized by activating mutations in *MYD88/CD79B*. We investigated whether *MYD88/CD79B* mutations could improve the classification and prognostication of diffuse large B-cell lymphomas.

In 250 primary diffuse large B-cell lymphomas, *MYD88/CD79B* mutations were identified by allele-specific PCR or next-generation-sequencing, *MYC/BCL2/BCL6* rearrangements were analyzed by FISH, and EBV was studied by EBER-ISH. Associations of molecular features with clinicopathologic characteristics, outcome, and prognosis according to International Prognostic Index were investigated.

*MYD88* and *CD79B* mutations were identified in 29.6% and 12.3%, *MYC*, *BCL2*, and *BCL6* rearrangements in 10.6%, 13.6%, and 20.3%, and EBV in 11.7% of diffuse large B-cell lymphomas, respectively. Prominent mutual exclusivity between EBV positivity, rearrangements, and *MYD88/CD79B* mutations established the value of molecular markers for recognition of biologically distinct diffuse large B-cell lymphoma subtypes. *MYD88*-mutated diffuse large B-cell lymphoma had a significantly inferior 5-year overall survival than wild-type *MYD88* diffuse large B-cell lymphoma (log-rank;  $P=0.019$ ). Diffuse large B-cell lymphoma without any of the studied aberrations had superior overall survival compared to cases carrying  $\geq 1$  aberrancy (log-rank;  $P=0.010$ ). *MYD88* mutations retained their adverse prognostic impact upon adjustment for other genetic and clinical variables by multivariable analysis and improved the prognostic performance of the International Prognostic Index.

This study demonstrates the clinical utility of defining *MYD88*-mutated diffuse large B-cell lymphoma as a distinct molecular subtype with adverse prognosis. Our data call for sequence analysis of *MYD88* in routine diagnostics of diffuse large B-cell lymphoma to optimize classification and prognostication, and to guide the development of improved treatment strategies.

## Introduction

Diffuse large B-cell lymphoma (DLBCL) is characterized by substantial heterogeneity in tumor biology and clinical behavior.<sup>1, 2</sup> Currently, rituximab, cyclophosphamide, doxorubicin, vincristine, and prednisone (R-CHOP) is used as a 'one-size-fits-all' treatment. Unfortunately, a considerable percentage of patients will experience chemorefractory disease or relapse, resulting in a 5-year overall survival (OS) of approximately 60%.<sup>3</sup> Particularly, patients with chemorefractory disease or an early relapse have a poor prognosis. For optimal counseling, DLBCL patients are categorized in risk groups according to the International Prognostic Index (IPI).<sup>4</sup> The IPI consists of clinical and biochemical parameters, but does not include tumor biological characteristics or provide any indication for precision medicine.<sup>5</sup>

The recently updated World Health Organization (WHO) classification of lymphoid neoplasms (2016) recognizes this heterogeneity by including selected drivers of lymphomagenesis for subclassification of DLBCL, i.e. the delineation of high-grade B-cell lymphomas (HGBL) with *MYC* and *BCL2* and/or *BCL6* rearrangements, and of Epstein-Barr virus-positive (EBV+) DLBCL.<sup>6</sup> *MYC*, *BCL2*, and *BCL6* rearrangements are found in respectively 4-14%, 20-30%, and ~20% of DLBCLs.<sup>7-9</sup> HGBLs comprise approximately 5-10% of all DLBCLs.<sup>9-11</sup> It is thought that the combination of *MYC*-stimulated cell proliferation and anti-apoptotic effects of *BCL2* in HGBL cause aggressive growth, relative resistance to therapy, and inferior OS.<sup>12</sup> In addition, Asian studies showed a frequency of 1-14% EBV positivity in DLBCLs and an association with inferior survival.<sup>13, 14</sup> EBV-associated viral proteins, such as latent membrane proteins (LMP)-1/2 and nuclear antigens, stimulate proliferation of B-cells via activation of nuclear factor-kappa-B (NF- $\kappa$ B), regulate immune evasion, and inhibit apoptosis.<sup>13</sup>

In the search for additional oncogenic drivers and to discriminate different molecular DLBCL subtypes, large next-generation-sequencing (NGS) studies have revealed specific mutational profiles that reflect the dysregulation of distinct intracellular pathways, including epigenetic regulation and NF- $\kappa$ B, Toll-like receptor (TLR), and B-cell receptor (BCR) signalling.<sup>1, 2, 15, 16</sup> Recurrent 'hotspot' mutations in *MYD88* (L265P) and *CD79B* (Y196) belong to the most prevalent sequence alterations in DLBCL. By altering the toll/interleukin-1 receptor domain of *MYD88*, the L265P increases interaction and consecutive phosphorylation of downstream targets, potentially without external stimuli from the TLR.<sup>17</sup> The connection of *MYD88* with BCR signalling within the so-called 'My-T-BCR' supercomplex facilitates activation of the NF- $\kappa$ B pathway via TLR9.<sup>2</sup> Hotspot mutations, such as Y196, in the *CD79B* subunit of the BCR lead to increased BCR expression and inhibition of feedback in the BCR signalling pathway by attenuating downstream Lyn kinase. Therefore, *CD79B* mutations are thought to contribute to lymphomagenesis by enhancing chronic active BCR signalling.<sup>18</sup>

Both *MYD88* and *CD79B* mutations are more prevalent in the so-called non-germinal center B-cell (GCB)-type DLBCL according to the cell-of-origin (COO) concept, originally developed based on

gene expression profiling.<sup>1, 2, 19</sup> In addition, the prevalence of these mutations varies greatly among DLBCL originating at different anatomical sites. We recently described a high percentage of *MYD88* L265P and *CD79B* Y196 mutations in intravascular large B-cell lymphomas (44% *MYD88* and 26% *CD79B*).<sup>20</sup> A high frequency of these mutations has also been found in other extranodal DLBCL, such as primary cutaneous DLBCL, leg type,<sup>21</sup> orbita/vitreoretinal DLBCL,<sup>22-24</sup> primary breast DLBCL,<sup>25</sup> and DLBCL presenting at immune-privileged (IP) sites, i.e. primary testicular DLBCL (PTL)<sup>26</sup> and primary central nervous system B-cell lymphoma (PCNSL).<sup>27-29</sup> Several studies have shown that *MYD88* mutations are associated with inferior OS in DLBCLs compared to wildtype *MYD88*.<sup>30, 31</sup>

Despite the increasing knowledge of the landscape of genetic drivers in DLBCL, the clinical implications of different oncogenic driver mutations remain unclear,<sup>32</sup> and the R-CHOP regimen is used as a uniform treatment. Since patients with chemorefractory disease or relapses after R-CHOP have a poor outcome, global 5-year OS in DLBCL is approximately 60%.<sup>3</sup> While HGBL patients have been recognized as a particularly unfavorable subgroup, prognostication for the remaining DLBCLs is based on clinical and biochemical parameters that define the IPI as well as primary extranodal manifestations.<sup>4, 5</sup> In contrast, the prognostic significance and interaction of mutations in *MYD88* and *CD79B* with standard molecular aberrations (as designated by the WHO 2016) have not yet been conclusively elucidated. Therefore, the present study investigated whether assessment of the mutational status of *MYD88* and *CD79B* would improve classification and prognostication of DLBCL.

## **Methods**

### **Patient cohort**

This retrospective study investigated a cohort of 250 primary DLBCLs. DLBCL patients were diagnosed between 2000-2016 at the Amsterdam University Medical Center, location AMC (AUMC), the Leiden University Medical Center (LUMC), and their affiliated hospitals. In all cases, diagnosis was centrally revised following the WHO classification 2008. A subset of this cohort was previously published without survival analysis.<sup>28, 29</sup> As our academic hospitals are tertiary referral centers, this cohort is enriched for IP locations. Formalin-fixed and paraffin-embedded (FFPE) tissue samples were obtained during standard diagnostic procedures. The study was performed in accordance with the Dutch Code for Proper Secondary Use of Human Tissue in accordance with the local institutional board requirements and the revised Declaration of Helsinki 2008 and was approved by the medical ethics committees of both the AUMC (W15\_213#15.0253) and the LUMC (B16.048). Patients were eligible in case tissue was available and *MYD88* mutational analysis was successful.

### **Histopathologic and molecular characterization**

In the majority, immunohistochemistry was performed for CD20, CD10, BCL6, MUM1, and BCL2. The Hans' algorithm was used for COO classification.<sup>33</sup> EBV status was assessed by EBV-encoded RNA *in situ* hybridization. *MYC*, *BCL2*, and *BCL6* rearrangements were analyzed by fluorescence *in situ* hybridization (FISH) using break-apart probes. Antibodies and probes are depicted in supplemental table-1.<sup>20, 29</sup> In the AUMC, DNA was isolated using the QIAamp DNA Micro kit (Qiagen) and mutational status of *MYD88* and *CD79B* was established by allele-specific PCR, followed by mutation-specific primers and confirmed by Sanger sequencing, as described before.<sup>28, 29</sup> In the LUMC, DNA isolation was automatically performed with the TPS robot (Siemens Healthcare Diagnostics), as presented previously.<sup>34</sup> The Ampliseq Cancer Hotspot Panel V.2-V.4 (Thermo Fisher Scientific) was used for detection of variants in *MYD88* (exons 3&5) and *CD79B* (exons 5&6). The minimum coverage threshold was 100 on-target reads with a minimum variant allele frequency of  $\geq 10\%$  of the reads. Variants were analyzed using Geneticist Assistant NGS Interpretative Workbench (v.1.4.15, SoftGenetics, State College). As described, identified variants were classified into five classes based upon potential pathogenicity and only class 4 (possibly pathogenic) and class 5 variants (pathogenic) were reported.<sup>35</sup>

### **Statistical analysis**

The correlation between clinicopathologic parameters and biological aberrations was examined with the Chi-square test or ANOVA. The Kaplan-Meier method was applied to estimate 5-year OS and progression free survival (PFS). The starting point for time-to-event analysis was date of histological diagnosis. An event for OS was defined as death by any cause. An event for PFS was



determined as relapse, disease progression, or death by any cause (whatever came first). If patients received palliative treatment and no remission evaluation was performed during follow-up, an event for progression was defined at 3 weeks before patients succumbed to their disease. Observational intervals of patients without any event at time of last follow up or at 5 years after diagnosis were censored. Median follow up time for the whole cohort was determined by use of reverse Kaplan-Meier.<sup>36</sup> The log-rank test was performed to compare risk groups. The Cox proportional-hazards model was used to estimate hazard ratios (HR) including 95% confidence intervals (95%-CI). Adjusted HRs were obtained in a multivariable Cox model. Competing risks analysis was used to estimate the cumulative incidences of relapse/progression, with non-relapse mortality considered as competing risk. Gray's test was performed to compare cumulative incidences, whereas a cause-specific Cox proportional-hazards model was used to estimate the impact of risk factors on them.<sup>37</sup> The incremental prognostic value of *MYD88* and/or *CD79B* was assessed by comparing Harrell's cross-validated C statistic for Cox models with and without *MYD88* and/or *CD79B*.<sup>38</sup> All statistical analyses were performed using SPSS software (version 23, IBM SPSS statistics) and RStudio (version 1.1442, RStudio, Inc. packages survival, prodlim, dynpred and cmprsk). P-values were two-sided and P<0.05 was considered statistically significant.

## **Results**

### **Patient characteristics**

Table-1 depicts the baseline characteristics of the 250 DLBCL patients (AUMC N=224 patients and LUMC N=26 cases). The median age at diagnosis was 61.4 years (range 18.6-89.6). A total of 38 DLBCL patients were immune-compromised, due to inherited conditions (severe combined immunodeficiency disorder, common variable immunodeficiency disorder), HIV infection, or extended use of therapeutic immunosuppression necessitated by organ transplantation or autoimmune disorders. Based on anatomical locations, 75 patients (30.0%) had strictly nodal DLBCL and in 67 patients (26.8%) the lymphoma presented in IP sites: 33 patients with PTL and 35 patients with PCNSL of whom one patient had testicular and CNS locations synchronously. The remaining 108 patients (43.2%) had extranodal disease in non-IP sites (with or without nodal involvement). With respect to staging, PCNSL was considered as advanced disease equivalent to Ann Arbor Stage IV for assignment of the IPI and subsequent statistical analyses. With this definition, 83 patients (33.5%) were categorized as having regional disease (Ann Arbor stage I-II) and 165 patients (66.5%) had advanced disease (stage III-IV). Sixty-one patients (25.3%) had an IPI risk score of 0/1, 148 patients (61.4%) an IPI of 2-3, and 32 patients (13.3%) an IPI of 4-5. The IPI of 9 patients was unknown. The majority of (extra)nodal and testicular DLBCL patients were treated with R-CHOP (N=160), CHOP (N=25), or (R)CHOP-like treatments (N=5) with curative intent. Curative treatment regimens incorporating high-dose methotrexate were initiated for 23 patients with PCNSL. Because of older age, poor clinical Eastern Cooperative Oncology Group Performance Status (ECOG-PS), or patients' refusal of treatment, 34 patients received palliative care only, mainly with steroids or (local) radiotherapy. The median follow up time was 6.6 years (range 0.1-15.7).<sup>36</sup>

### **Molecular characterization: mutated *MYD88* discriminates a distinct DLBCL subgroup**

According to the Hans' algorithm, DLBCLs were classified as GCB (N=100, 40.0%), non-GCB (N=130, 52.0%), or unclassifiable (N=20, 8.0%), with no statistical difference between nodal, extranodal, and IP locations (P=0.228)(table 2).<sup>33</sup>

In 198 patients (79.2%), molecular analysis for *MYD88* and *CD79B* mutations, *MYC*, *BCL2*, and *BCL6* rearrangements, and EBV infection was complete, whereas in 52 patients, partial data sets were available (figure-1; table-2). *MYD88* mutations were identified in 74 cases (29.6%), of whom 67 harbored the hotspot L265P mutation. The other *MYD88* variants were S219C (N=5) and S243N (N=2). In line with a published meta-analysis,<sup>30</sup> mutated *MYD88* was significantly correlated to older age ( $\geq 65$  years), anatomical lymphoma location, and non-GCB subtype (P=0.006; P<0.001; P=0.042, respectively). *CD79B* mutations were detected in 29 patients (12.3%), including the hotspot Y196 mutation (N=28) and the L188 mutation (N=2, one patient had both mutations). *MYC*, *BCL2*, and *BCL6*

were rearranged in 23 (10.6%), 30 (13.6%), and 44 (20.3%) DLBCLs, respectively, with a total of nine HGBL patients (4.1%).

As suggested by previous reports and other studies, *MYD88* and *CD79B* mutations were significantly more common in IP-DLBCL (67.2% resp. 25.8%) compared to nodal (17.3% resp. 4.1%) and other extranodal sites (14.8% resp. 9.3%) ( $P < 0.001$  and  $P < 0.001$ ).<sup>26, 29, 39</sup> In contrast, *BCL2* rearrangements were more prevalent in nodal and extranodal DLBCL ( $P = 0.001$ ), whereas *MYC* and *BCL6* rearrangements were evenly distributed across the anatomical sites. EBV was positive in 28 patients (11.7%) and was not associated with anatomical location ( $P = 0.091$ ).

In the 198 cases with complete molecular analysis, hardly any overlap between the presence of oncogenic rearrangements, EBV positivity, or *MYD88* and/or *CD79B* mutations was observed (figure-2A), suggesting that they represent distinct DLBCL subgroups with different drivers of lymphomagenesis. *CD79B* mutations co-occurred with *MYD88* mutations in 18 of 23 cases (78.2%). In contrast, *MYD88* mutations co-occurred with any rearrangement in only seven of 60 patients (11.7%) and with EBV positivity in only one case (1.7%). EBV infection was detected in only three out of 71 cases (4.2%) with a rearrangement. In 51 patients (25.8%) with full molecular characterization, no aberrancy was detected.

#### **Mutated MYD88 predicts inferior survival**

All outcomes are reported at 5-year survival. For the entire cohort, OS was 61.0% (95%-CI 55.1-67.5) and PFS was 52.6% (95%-CI 46.6-59.3). Cumulative incidences of relapse/progression and non-relapse mortality were 37.2% (95%-CI 31.2-43.3) and 10.1% (95%-CI 6.4-13.9), respectively. Figure-3 shows survival outcomes presented for anatomical location, IPI-score, and *MYD88* status. Survival outcomes of COO and the other aberrations are outlined in supplemental figure-2 (none of these factors had a significant impact).

The IPI clearly predicted OS (figure-3): patients with IPI scores of 0/1, 2/3, and 4/5 had an OS of 84.9% (95%-CI 76.3-94.5), 58.0% (95%-CI 50.3-66.8), and 34.4% (95%-CI 21.3-55.5), respectively. IPI also showed a significant difference in cumulative incidences of relapses (Gray's;  $P = 0.025$ ) and non-relapse mortality (Gray's;  $P = 0.006$ ). In addition to the IPI, DLBCL with IP locations had inferior outcomes (OS 47.1%, 95%-CI 36.5-60.9; PFS 41.0%, 95%-CI 30.7-54.9) compared to nodal (OS 71.2%, 95%-CI 61.4-82.4; PFS 55.7%, 95%-CI 45.3-68.6) and other extranodal sites (OS 62.6%, 95%-CI 53.9-72.7; PFS 58.1%, 95%-CI 49.4-68.2) (log-rank;  $P = 0.004$  and  $P = 0.024$ ). This unfavorable prognosis was particularly associated with CNS location. Within the IP group, patients with CNS location had a significant inferior 5-year OS of 29.9% (95%-CI 17.7-50.5) compared to 65.5% (95%-CI 50.9-84.3%) for PTL (log-rank;  $P = 0.003$ ).

With respect to molecular markers, patients without any detected aberrancy demonstrated a good-risk profile with superior OS (78.0%, 95%-CI 67.2-90.4, versus 56.3%, 95%-CI:48.6-65.2; figure-

2B) (log-rank; P=0.010) and PFS (65.4%, 95%-CI 53.2-80.3, versus 48.2%, 95%-CI 40.6-57.3; figure-2C) (log-rank; P=0.031) compared to patients who had one or more aberration(s). The cumulative incidence of relapse/progression for this good-risk profile was 28.6% (95%-CI 15.8-41.4) compared to 39.3% (95%-CI 31.2-47.4) (Gray's; P=0.155). This good risk profile included patients with lower ECOG-PS, age<60 years, and more GCB subtypes (Chi square; P=0.012, P=0.001, and P=0.006, respectively) compared to patients with one or more aberrations. Patients in the good risk category seem to be susceptible for immune-chemotherapy with enduring responses, however, the molecular background of this subgroup remains unknown. In IP-DLBCL, a total of 93.8% of the patients were classified in the risk group with  $\geq 1$  aberrations.

*MYD88*-mutated DLBCLs had a significantly inferior 5-year OS compared to DLBCL with wildtype *MYD88* (log-rank; P=0.019; HR 1.64, 95%-CI 1.08-2.48) and significantly inferior 5-year PFS (log-rank; P=0.049; HR 1.46, 95%-CI 1.00-2.14). Employing competing risk analysis, *MYD88*-mutated DLBCLs revealed significantly higher relapse rates (46.6%, 95%-CI 35.1-58.1) than cases with wildtype *MYD88* (33.3%, 95%-CI 26.2-40.4)(Gray's; P=0.029; CSH 1.62, 95%-CI 1.06-2.48), while non-relapse mortality showed no significant difference (Gray's; P=0.832). Mutated *CD79B* showed higher cumulative incidence for relapse/progression (56.3%, 95%-CI 37.9-74.8) versus wildtype *CD79B* (35.1%, 95%-CI 28.5-41.8)(Gray's; P=0.019, CSH: 1.82, 95%-CI 1.06-3.14), whereas no significant difference was found for OS (HR 1.43, 95%-CI 0.81-2.53).

Despite relatively high HRs, none of the other molecular aberrations was a significantly adverse prognostic factor for OS (table-3), which can be explained by lack of power due to the low incidence of these aberrations. For these molecular data, univariate cause-specific hazards for relapse/progression showed similar results. The nine HGBLs had an OS of 50.0% (95%-CI 24.1-100) compared to 63.6% (95%-CI 57.3-70.6) (log-rank; P=0.628) for non-HGBLs.

### **Prognostic significance of *MYD88* mutations in multivariable analysis**

To evaluate the prognostic impact of mutated *MYD88* on survival outcomes in addition to other molecular aberrations and the IPI, the initial multivariable Cox regression model included the standard individual IPI risk factors (Model 1, table-3A/3B). In the second model, the current WHO 2016 molecular aberrations (EBV and oncogenic rearrangements) were added. In the third model, also *MYD88* and *CD79B* mutations were included. *MYD88* mutations showed prognostic significance for OS (HR 1.87, 95%-CI 1.10-3.20) in addition to ECOG-PS ( $\geq 2$ ) (HR 8.16, 95%-CI 4.90-13.59) and Ann Arbor stage (III/IV) (HR 1.84, 95%-CI 1.04-3.25). In this third model, oncogenic rearrangements, mutated *CD79B*, elevated LDH, and age (>65 years) did not have a significant impact. The performance of the IPI prognostic model was improved by adding all molecular aberrations and mutated *MYD88* and *CD79B* as risk factors, as indicated by an increase in cross-validated C-index (CVC) from 0.67 to 0.70. *MYD88* did not have significant impact on cause-specific survival (HR 1.42,

95%-CI 0.85-2.37), whilst ECOG-PS, Ann Arbor stage, and extranodal location were prognostic in this model.

Further multivariable analyses were performed to evaluate the prognostic significance of *MYD88* mutational status in comparison to COO subtype or anatomical lymphoma location. COO subtype did not improve the performance of models 2 and 3 (results not shown). However, the prognostic impact of model 2 was improved by adding anatomical lymphoma location (CVC index = 0.71, model 4, presented in supplemental table-1) and outperforms model 2 (table-3A, CVC index = 0.69, including the IPI factors and molecular aberrations of WHO 2016). Model 4 demonstrated a nearly identical prognostic performance when compared to model 3 (CVC index = 0.70, including the IPI factors, molecular aberrations of WHO 2016 and the mutational status of *MYD88* and *CD79B*). When adding the mutational status of *MYD88* and *CD79B* to model 4, the performance of this model 5 was not improved (CVC index 0.71, supplemental table-1). As such, the prognostic impact of the *MYD88* mutational status on mortality was not superior to anatomical lymphoma location.

Next, we explored whether mutated *MYD88* could improve the prognostic performance of the currently used IPI risk model (table-4). Inclusion of the IPI as continuous variable (0-5 points) and the *MYD88* status in the multivariable analysis demonstrated an independent and similar impact of mutated *MYD88* (HR 1.83, 95%-CI 1.19-2.80) and IPI (HR 1.77, 95%-CI 1.47-2.13) on OS. Similar effects were observed for cause-specific survival (table-4). For the models OS and relapse/progression, an increase in CVC-index was observed from 0.57 to 0.61 and 0.53 to 0.57, respectively. Altogether, these multivariable survival analyses demonstrated the significant prognostic importance of mutated *MYD88*, next to (genetic) aberrations and clinical/biochemical variables, and the improvement of adding mutated *MYD88* to the prognostic performance of the IPI.

To evaluate possible confounding of the impact of mutated *MYD88* and the outcomes by anatomical lymphoma location, we performed a sensitivity analysis for OS on the cohort stratified by anatomical lymphoma location, including CNS involvement. For patients with CNS involvement (N=35), *MYD88* had an unadjusted HR of 1.94 (95%-CI 0.77-4.90) in univariable analysis. For patients without CNS involvement (N=215), *MYD88* did not have a significant impact on OS with an adjusted HR of 1.81 (95%-CI 0.96-3.42), when applying multivariable analysis as described for model-3 (table-3B). Although not statistically significant, the adjusted HR for this subgroup was similar to the original HR for the entire cohort.

## **Discussion**

To the best of our knowledge, this is the first study evaluating the clinical significance of mutated *MYD88* and *CD79B* in DLBCL, in addition to the oncogenic drivers that are currently included in the WHO classification 2016 (EBV status and *MYC*, *BCL2*, and *BCL6* rearrangements), the IPI risk factors, and well-defined anatomical locations.

The strength of this study is the large number of patients with good clinical annotation and complete molecular analysis (N=198). In addition, our study shows that the incorporation of mutational status of *MYD88* into a clinical/biochemical risk score as the IPI is feasible. An increase in the predictive performance of the IPI risk model as is illustrated by an increase in CVC-index, suggests that this model can be improved by the introduction of molecular aberrations. However, interpreting the results, we have encountered several limitations. *MYD88*-mutated DLBCLs more often had extranodal location, older age (and thus a high IPI), and non-GCB subtype. Therefore, these patients were more frequently subjected to palliative care. Possibly interaction between treatment and mutated *MYD88* has not been tested as more data is needed. We present an average effect over different treatment modalities. Since reported frequencies and survival outcomes are similar to previous literature, our cohort appears to be representative for the target population.<sup>3, 7-9, 13</sup> To investigate the prognostic significance of mutated *MYD88* adjusted for the IPI for the entire cohort, we considered PCNSL as advanced disease stage, although it is not common practice to apply the IPI in PCNSL patients. Additionally, our cohort is enriched for IP locations. Therefore, a sensitivity analysis was performed excluding PCNSL patients, demonstrating that the adjusted HR of *MYD88* for OS was similar to the entire cohort. This indicates that our results are not affected by confounding by CNS localisation. Hence, we believe that our data corroborate the clinical relevance of mutant *MYD88* for diagnostic classification and prognostication of DLBCL and support implementation of *MYD88* mutational analysis in routine diagnostics. The simplicity and accessibility to examine *MYD88* mutations and associated low costs permit an efficient timely implementation. In addition, *CD79B* mutations were prognostic in univariate analysis, but when adjusted for other aberrations in the multivariable analysis the prognostic importance disappeared. This finding may be explained by the prominent overlap between *MYD88* and *CD79B* mutations, as 78.2% of mutated *CD79B* had co-occurring *MYD88* mutations.

An important result of our study is the recognition of prominent mutual exclusivity between the presence of mutations in *MYD88* and/or *CD79B*, *MYC*, *BCL2*, and *BCL6* rearrangements, and EBV infection, indicating that *MYD88* and/or *CD79B*-mutated tumors present a distinct DLBCL subcategory. In accordance with a large meta-analysis and two other studies,<sup>30, 40, 41</sup> *MYD88* L265P mutations were preferentially found in specific anatomical sites (e.g. testis and CNS) and were significantly associated with non-GCB subtypes, older age, and poor OS. However, the published literature study did not explicitly analysed IP sites, nor evaluated the interaction of *MYD88* mutations

with EBV status or oncogenic rearrangements in multivariable analysis. Other NGS studies have recently demonstrated high frequencies of mutated *MYD88* (15-18%) in large cohorts of DLBCLs.<sup>1, 2, 15, 42-44</sup> Besides a certain association of mutated *MYD88* with poor OS (e.g. in non-GCB DLBCL), cluster analysis of multiple genes indicated distinct DLBCL subentities, including mutated *MYD88* as an important classifier for NF- $\kappa$ B pathway activation. Again, these NGS studies did not take into account specific anatomical sites or investigated the interaction and prognostic significance of mutated *MYD88* in correlation with EBV status or *MYC*, *BCL2*, and *BCL6* rearrangements.

In this context, our study adds important new knowledge by demonstrating *MYD88* mutations as an adverse prognostic factor for OS and relapse/progression in a multivariate analysis that takes all major known clinical and WHO classification-defined risk factors into account. This insight does not only show that the incorporation of mutational status of *MYD88* into a clinical/biochemical risk score as the IPI is feasible, but also highlights the importance of assessing *MYD88* at time of diagnosis for optimal classification and patient counselling. An increase in the predictive performance of the IPI risk model, as is illustrated by an increase in CVC-index, formally suggests that this model can be improved by the introduction of molecular aberrations. However, the prognostic impact of the *MYD88* mutational status on the presented multivariable models was not superior to anatomical lymphoma location. Whether the *MYD88* mutational status outperforms the predictive performance of anatomical lymphoma location in the described prognostic models needs further validation in an external cohort. Of note, no difference was found for non-relapse mortality, indicating that mutated *MYD88* is a lymphoma-specific poor prognostic factor. Routine diagnostic assessment of *MYD88* mutations is likely to gain decisive importance for DLBCL since several approaches may therapeutically target *MYD88*.<sup>45</sup> Several studies have indicated that DLBCLs with mutated *MYD88* and/or *CD79B* are more sensitive to Bruton's Tyrosine Kinase (BTK)-inhibitors.<sup>46-48</sup> As such, objective analysis of *MYD88* mutations will not only improve diagnostic classification and prognostication, but might also enable patient selection for precision medicine such as with BTK-inhibitors. However, the predictive significance of mutated *MYD88* with or without *CD79B* mutations needs to be validated in upcoming clinical trials, including precision medicine targeting the BCR and TLR cascades.

Finally, as a corollary of this study, we identified a novel good risk DLBCL group characterized by the absence of detected genetic aberrations. These DLBCLs appeared to be highly sensitive to standard immune-chemotherapy as first-line treatment. Future studies, employing a larger NGS targeted gene panel, may elucidate the genetic drivers in this group. We anticipate that there might be a parallel with the study of Chapuy *et al.*,<sup>15</sup> which identified a good-risk DLBCL group harbouring mainly aberrations in epigenetic pathways.

Studies by Rossi *et al.* and Kurtz *et al.*,<sup>49, 50</sup> have analysed liquid biopsies in DLBCLs demonstrating that the mutational load in circulating-free tumor DNA obtained by NGS technologies reliably mirror the mutational profiles of DLBCL tissues, including mutated *MYD88*. Additionally,

digital droplet PCR techniques enable the quantification of low amounts of mutated *MYD88* in any physiological fluid.<sup>51</sup> Further investigation is needed to determine whether the analysis of mutated *MYD88* in liquid biopsies prior to and during therapy will be significantly predictive for treatment response and to establish its specificity and sensitivity.

## **Conclusion**

The present study demonstrates that the presence of *MYD88* and *CD79B* mutations is almost mutually exclusive with EBV infection and *MYC*, *BCL2*, and *BCL6* rearrangements, indicating distinctive molecular DLBCL subgroups that can be readily appreciated in clinical practice. Mutant *MYD88* showed its prognostic importance for inferior survival outcomes, even next to other genetic and clinical prognosticators and IPI. Additionally, patients lacking all analysed aberrancies represented a novel risk group with superior survival outcomes. Taken together and after validation in an independent cohort, these results provide a rationale for including *MYD88* mutational analysis in the routine diagnostics of DLBCL, to improve classification and prognostication, as well as to guide future treatment strategies.



## References

1. Reddy A, Zhang J, Davis NS, et al. Genetic and Functional Drivers of Diffuse Large B Cell Lymphoma. *Cell*. 2017;171(2):481-494 e415.
2. Phelan JD, Young RM, Webster DE, et al. A multiprotein supercomplex controlling oncogenic signalling in lymphoma. *Nature*. 2018;560(7718):387-391.
3. Cunningham D, Hawkes EA, Jack A, et al. Rituximab plus cyclophosphamide, doxorubicin, vincristine, and prednisolone in patients with newly diagnosed diffuse large B-cell non-Hodgkin lymphoma: a phase 3 comparison of dose intensification with 14-day versus 21-day cycles. *Lancet*. 2013;381(9880):1817-1826.
4. A predictive model for aggressive non-Hodgkin's lymphoma. *N Engl J Med*. 1993;329(14):987-994.
5. Wight JC, Chong G, Grigg AP, Hawkes EA. Prognostication of diffuse large B-cell lymphoma in the molecular era: moving beyond the IPI. *Blood Rev*. 2018;32(5):400-415.
6. Swerdlow SH, Campo E, Pileri SA, et al. The 2016 revision of the World Health Organization classification of lymphoid neoplasms. *Blood*. 2016;127(20):2375-2390.
7. Rosenthal A, Younes A. High grade B-cell lymphoma with rearrangements of MYC and BCL2 and/or BCL6: Double hit and triple hit lymphomas and double expressing lymphoma. *Blood Rev*. 2017;31(2):37-42.
8. Shustik J, Han G, Farinha P, et al. Correlations between BCL6 rearrangement and outcome in patients with diffuse large B-cell lymphoma treated with CHOP or R-CHOP. *Haematologica*. 2010;95(1):96-101.
9. Schmidt-Hansen M, Berendse S, Marafioti T, McNamara C. Does cell-of-origin or MYC, BCL2 or BCL6 translocation status provide prognostic information beyond the International Prognostic Index score in patients with diffuse large B-cell lymphoma treated with rituximab and chemotherapy? A systematic review. *Leuk Lymphoma*. 2017;58(10):2403-2418.
10. Akyurek N, Uner A, Benekli M, Barista I. Prognostic significance of MYC, BCL2, and BCL6 rearrangements in patients with diffuse large B-cell lymphoma treated with cyclophosphamide, doxorubicin, vincristine, and prednisone plus rituximab. *Cancer*. 2012;118(17):4173-4183.
11. McPhail ED, Maurer MJ, Macon WR, et al. Inferior survival in high-grade B-cell lymphoma with MYC and BCL2 and/or BCL6 rearrangements is not associated with MYC/IG gene rearrangements. *Haematologica*. 2018;103(11):1899-1907.
12. Leskov I, Pallasch CP, Drake A, et al. Rapid generation of human B-cell lymphomas via combined expression of Myc and Bcl2 and their use as a preclinical model for biological therapies. *Oncogene*. 2013;32(8):1066-1072.
13. Gao X, Li J, Wang Y, Liu S, Yue B. Clinical characteristics and prognostic significance of EBER positivity in diffuse large B-cell lymphoma: A meta-analysis. *PLoS One*. 2018;13(6):e0199398.
14. Lu TX, Liang JH, Miao Y, et al. Epstein-Barr virus positive diffuse large B-cell lymphoma predict poor outcome, regardless of the age. *Sci Rep*. 2015;5:12168.
15. Chapuy B, Stewart C, Dunford AJ, et al. Molecular subtypes of diffuse large B cell lymphoma are associated with distinct pathogenic mechanisms and outcomes. *Nat Med*. 2018;24(5):679-690.
16. Schmitz R, Wright GW, Huang DW, et al. Genetics and Pathogenesis of Diffuse Large B-Cell Lymphoma. *N Engl J Med*. 2018;378(15):1396-1407.
17. Ngo V.N. Young RM, Schmitz R, et al. Oncogenically active *MYD88* mutations in human lymphoma. *Nature*. 2011;470(7332):115-119.
18. Davis RE, Ngo VN, Lenz G, et al. Chronic active B-cell-receptor signalling in diffuse large B-cell lymphoma. *Nature*. 2010;463(7277):88-92.
19. Alizadeh AA, Eisen MB, Davis RE, et al. Distinct types of diffuse large B-cell lymphoma identified by gene expression profiling. *Nature*. 2000;403(6769):503-511.
20. Schrader AMR, Jansen PM, Willemze R, et al. High prevalence of MYD88 and CD79B mutations in intravascular large B-cell lymphoma. *Blood*. 2018;131(18):2086-2089.
21. Zhou XA, Louissaint A, Jr., Wenzel A, et al. Genomic Analyses Identify Recurrent Alterations in Immune Evasion Genes in Diffuse Large B Cell Lymphoma, Leg Type. *J Invest Dermatol*. 2018;138(11):2365-2376.

22. Bonzheim I, Giese S, Deuter C, et al. High frequency of MYD88 mutations in vitreoretinal B-cell lymphoma: a valuable tool to improve diagnostic yield of vitreous aspirates. *Blood*. 2015;126(1):76-79.
23. Cani AK, Soliman M, Hovelson DH, et al. Comprehensive genomic profiling of orbital and ocular adnexal lymphomas identifies frequent alterations in MYD88 and chromatin modifiers: new routes to targeted therapies. *Mod Pathol*. 2016;29(7):685-697.
24. Raja H, Salomao DR, Viswanatha DS, Pulido JS. Prevalence of Myd88 L265p Mutation in Histologically Proven, Diffuse Large B-Cell Vitreoretinal Lymphoma. *Retina*. 2016;36(3):624-628.
25. Taniguchi K, Takata K, Chuang SS, et al. Frequent MYD88 L265P and CD79B Mutations in Primary Breast Diffuse Large B-Cell Lymphoma. *Am J Surg Pathol*. 2016;40(3):324-334.
26. Kraan W, van Keimpema M, Horlings HM, et al. High prevalence of oncogenic MYD88 and CD79B mutations in primary testicular diffuse large B-cell lymphoma. *Leukemia*. 2014;28(3):719-720.
27. Chapuy B, Roemer MG, Stewart C, et al. Targetable genetic features of primary testicular and primary central nervous system lymphomas. *Blood*. 2016;127(7):869-881.
28. Kersten MJ, Kraan W, Doorduijn J, et al. Diffuse large B cell lymphomas relapsing in the CNS lack oncogenic MYD88 and CD79B mutations. *Blood Cancer J*. 2014;4:e266.
29. Kraan W, Horlings HM, van Keimpema M, et al. High prevalence of oncogenic MYD88 and CD79B mutations in diffuse large B-cell lymphomas presenting at immune-privileged sites. *Blood Cancer J*. 2013;3:139.
30. Lee JH, Jeong H, Choi JW, Oh H, Kim YS. Clinicopathologic significance of MYD88 L265P mutation in diffuse large B-cell lymphoma: a meta-analysis. *Sci Rep*. 2017;7(1):1785.
31. Yu S, Luo H, Pan M, et al. High frequency and prognostic value of MYD88 L265P mutation in diffuse large B-cell lymphoma with R-CHOP treatment. *Oncol Lett*. 2018;15(2):1707-1715.
32. Vermaat JS, Pals ST, Younes A, et al. Precision medicine in diffuse large B-cell lymphoma: hitting the target. *Haematologica*. 2015;100(8):989-993.
33. Hans CP, Weisenburger DD, Greiner TC, et al. Confirmation of the molecular classification of diffuse large B-cell lymphoma by immunohistochemistry using a tissue microarray. *Blood*. 2004;103(1):275-282.
34. van Eijk R, Stevens L, Morreau H, van Wezel T. Assessment of a fully automated high-throughput DNA extraction method from formalin-fixed, paraffin-embedded tissue for KRAS, and BRAF somatic mutation analysis. *Exp Mol Pathol*. 2013;94(1):121-125.
35. Sibinga Mulder BG, Mieog JS, Handgraaf HJ, et al. Targeted next-generation sequencing of FNA-derived DNA in pancreatic cancer. *J Clin Pathol*. 2017;70(2):174-178.
36. Schemper M, Smith TL. A note on quantifying follow-up in studies of failure time. *Control Clin Trials*. 1996;17(4):343-346.
37. Kim HT. Cumulative incidence in competing risks data and competing risks regression analysis. *Clin Cancer Res*. 2007;13(2 Pt 1):559-565.
38. Houwelingen HC PH. *Dynamic Prediction in Clinical Survival Analysis*. Chapman & Hall. 2012.
39. Zheng M, Perry AM, Bierman P, et al. Frequency of MYD88 and CD79B mutations, and MGMT methylation in primary central nervous system diffuse large B-cell lymphoma. *Neuropathology*. 2017;37(6):509-516.
40. Rovira J. KK, Valera A., et al. . MYD88 L265P mutations, but no other variants, identify a subpopulation of DLBCL patients of activated B-cell origin, extranodal involvement, and poor outcome. *Clin Cancer Res*. 2016;22(11):10.
41. Dubois S, Viailly PJ, Bohers E, et al. Biological and Clinical Relevance of Associated Genomic Alterations in MYD88 L265P and non-L265P-Mutated Diffuse Large B-Cell Lymphoma: Analysis of 361 Cases. *Clin Cancer Res*. 2017;23(9):2232-2244.
42. Intlekofer AM, Joffe E, Batlevi CL, et al. Integrated DNA/RNA targeted genomic profiling of diffuse large B-cell lymphoma using a clinical assay. *Blood Cancer J*. 2018;8(6):60.
43. Karube K, Enjuanes A, Dlouhy I, et al. Integrating genomic alterations in diffuse large B-cell lymphoma identifies new relevant pathways and potential therapeutic targets. *Leukemia*. 2018;32(3):675-684.
44. Xu PP, Zhong HJ, Huang YH, et al. B-cell Function Gene Mutations in Diffuse Large B-cell Lymphoma: A Retrospective Cohort Study. *EBioMedicine*. 2017;16:106-114.

45. Yu X, Li W, Deng Q, et al. MYD88 L265P Mutation in Lymphoid Malignancies. *Cancer Res.* 2018;78(10):2457-2462.
46. Grommes C, Pastore A, Palaskas N, et al. Ibrutinib Unmasks Critical Role of Bruton Tyrosine Kinase in Primary CNS Lymphoma. *Cancer Discov.* 2017;7(9):1018-1029.
47. Lionakis MS, Dunleavy K, Roschewski M, et al. Inhibition of B Cell Receptor Signaling by Ibrutinib in Primary CNS Lymphoma. *Cancer Cell.* 2017;31(6):833-843.
48. Wilson WH, Young RM, Schmitz R, et al. Targeting B cell receptor signaling with ibrutinib in diffuse large B cell lymphoma. *Nat Med.* 2015;21(8):922-926.
49. Kurtz DM, Scherer F, Jin MC, et al. Circulating Tumor DNA Measurements As Early Outcome Predictors in Diffuse Large B-Cell Lymphoma. *J Clin Oncol.* 2018;36(28):2845-2853.
50. Rossi D, Diop F, Spaccarotella E, et al. Diffuse large B-cell lymphoma genotyping on the liquid biopsy. *Blood.* 2017;129(14):1947-1957.
51. Hiemcke-Jiwa LS, Minnema MC, Radersma-van Loon JH, et al. The use of droplet digital PCR in liquid biopsies: A highly sensitive technique for MYD88 p.(L265P) detection in cerebrospinal fluid. *Hematol Oncol.* 2018;36(2):429-435.

**Table 1 – Patient characteristics at time of diagnosis**

	<b>All patients (N = 250)</b>
Gender	
Male	168 (67.2 %)
Female	82 (32.8 %)
Median age in years (range)	61.4 (18.6-89.6)
History of immune deficiency	38 (15.2 %)
HIV	16 (6.4 %)
Organ transplantation with prolonged use of immune suppressive drugs	7 (2.8 %)
SCID/CVID	3 (1.2 %)
Other <sup>a</sup>	13 (5.2 %)
Anatomical lymphoma location	
Nodal	75 (30.0 %)
Extranodal <sup>b</sup> (with or without nodal location)	108 (43.2 %)
Immune-privileged	67 (26.8 %)
CNS location <sup>c</sup>	35 (14.0 %)
Testis location	32 (13.2 %)
Ann Arbor <sup>d</sup>	(N = 248)
I	51 (20.6 %)
II	32 (12.9 %)
III	26 (10.5 %)
IV	139 (56.0 %)
IPI <sup>d</sup>	(N = 241)
0	20 (8.3 %)
1	41 (17.0 %)
2	90 (37.3 %)
3	58 (24.1 %)
4	24 (10.0 %)
5	8 (3.3 %)
First line treatment	
R-CHOP	160 (64.0 %)
CHOP	25 (10.0 %)
Other chemotherapy <sup>e</sup>	5 (2.0 %)
Radiotherapy only	1 (0.4 %)
Surgery only	2 (0.8 %)
None / Palliative	34 (13.6 %)
High-dose methotrexate regimens (HD-MTX) <sup>f</sup>	23 (9.2 %)
Radiotherapy	77 (30.8 %)
With curative intent	60 (24.0 %)
Palliative care only	17 (6.8 %)
Response to first line treatment	
Complete response	166 (66.4 %)
Partial response	14 (5.6 %)
Stable disease	2 (0.8 %)
Progressive disease	67 (26.8 %)
Too early to call	1 (0.4 %)

Abbreviations: HIV – Human Immunodeficiency Virus; SCID – Severe Combined Immunodeficiency Disorder; CVID – Common Variable Immunodeficiency Disorder; CNS – Central Nervous System; IPI – International Prognostic Index; (R-)CHOP – (rituximab), cyclophosphamide, doxorubicin, vincristine, prednisone.

<sup>a</sup> Others include inflammatory bowel disease, Sjögren, sarcoidosis, atopic dermatitis, and/or auto-immune haemolytic anaemia.

<sup>b</sup> Extranodal comprised lung, liver, spleen, bone marrow, breast, soft tissue, thyroid, bone, (ad)renal, orbital, stomach, skin, pancreas, bowel, bladder, ovary, and naso-/oropharynx locations.

<sup>c</sup> One patient experienced both CNS and testicular locations.

<sup>d</sup> PCNSL were classified as advanced stage (Ann-Arbor stage IV) and subsequently received one risk point for IPI.

<sup>e</sup> (R-)C(E)OP: (rituximab), cyclophosphamide, (etoposide), vincristin, prednisone.

<sup>f</sup> Specific regimens include HD-MTX + cytarabine + carmustine, HD-MTX + cytarabine, rituximab + HD-MTX + prednisone (RMP), cyclophosphamide + doxorubicin + teniposide + prednisone + vincristine + bleomycin (CHVMP/BV), HD-MTX + procarbazine + lomustine, HD-MTX + cytarabine + thiotepa + rituximab (MATRiX), HD-MTX + teniposide + carmustin + prednisone (MBVP) (+ rituximab).

**Table 2 – Hans' algorithm and molecular analysis at time of diagnosis**

	All patients (N = 250)	Nodal (N = 75)	Extranodal with/without nodal (N = 108)	Immune- privileged (N = 67)	P*
Cell-of-origin, according to Hans' algorithm (N=250)					0.228
GCB	100 (40.0 %)	36 (48.0 %)	38 (58.3 %)	26 (38.8%)	
Non-GCB	130 (52.0 %)	35 (46.7 %)	63 (35.2 %)	32 (47.8 %)	
Unclassifiable	20 (8.0 %)	4 (5.3 %)	7 (6.5 %)	9 (13.4 %)	
<i>MYD88</i> (N=250)					<0.001
Wildtype	176 (70.4 %)	62 (82.7 %)	92 (85.2 %)	22 (32.8 %)	
Mutated	74 (29.6 %)	13 (17.3 %)	16 (14.8 %)	45 (67.2 %)	
<i>CD79B</i> (N=236)					<0.001
Wildtype	207 (87.7 %)	70 (95.9 %)	88 (90.7 %)	49 (74.2 %)	
Mutated	29 (12.3 %)	3 (4.1 %)	9 (9.3 %)	17 (25.8 %)	
<i>MYC</i> (N=217)					0.434
Wildtype	194 (89.4 %)	59 (85.5 %)	89 (90.8 %)	46 (92.0 %)	
Rearranged	23 (10.6 %)	10 (14.5 %)	9 (9.2 %)	4 (8.0 %)	
<i>BCL2</i> (N=221)					0.001
Wildtype	191 (86.4 %)	53 (74.6 %)	89 (89.9 %)	49 (96.1 %)	
Rearranged	30 (13.6 %)	18 (25.4 %)	10 (10.1 %)	2 (3.9 %)	
<i>BCL6</i> (N=217)					0.675
Wildtype	173 (79.7 %)	57 (82.6 %)	78 (79.6 %)	38 (76.0 %)	
Rearranged	44 (20.3 %)	12 (17.4 %)	20 (20.4 %)	12 (24.0 %)	
High grade B-cell lymphoma (N=221)					0.686
Negative	212 (95.9 %)	66 (95.7 %)	98 (97.0 %)	48 (94.1 %)	
Positive	9 (4.1 %)	3 (4.3 %)	3 (3.0 %)	3 (5.9 %)	
EBV status (N=239)					0.091
Negative	211 (88.3 %)	65 (89.0 %)	88 (83.8 %)	58 (95.1 %)	
Positive	28 (11.7 %)	8 (11.0 %)	17 (16.2 %)	3 (4.9 %)	
Genetic aberrations (N=198)					0.002
None	51 (25.8 %)	21 (31.8 %)	27 (32.1 %)	3 (6.3 %)	
One or more	147 (74.2 %)	45 (68.2 %)	57 (67.9 %)	45 (93.8 %)	

Abbreviations: EBV – Epstein-Barr Virus.

\* P-value indicating a difference in distribution between the three subgroups as calculated by Pearson's Chi Square test. The number between brackets in the left-hand column represents the number of patients from whom this information was available.

**Table 3A – Prognostic impact of molecular aberrations and IPI risk factors on overall survival: univariable and multivariable analysis**

	Overall survival							
	Univariable		Multivariable Model 1 (IPI)		Multivariable Model 2 (IPI + molecular aberrations WHO 2016)		Multivariable Model 3 (IPI + molecular aberrations WHO 2016 + MYD88 + CD79B)	
	HR	95%-CI	HR	95%-CI	HR	95%-CI	HR	95%-CI
IPI: >2 Extranodal Yes (vs No)	1.37	0.91-2.07	1.41	0.90-2.22	1.49	0.94-2.37	<b>1.71</b>	1.07-2.74
IPI: Stage III/IV (vs I/II)	<b>2.33</b>	1.41-3.85	1.67	0.98-2.84	1.71	0.97-3.00	<b>1.84</b>	1.04-3.25
IPI: ECOG Performance Score >2 (vs <1)	<b>8.15</b>	5.23-12.7	<b>7.53</b>	4.67-12.15	<b>8.69</b>	5.23-14.45	<b>8.16</b>	4.90-13.59
IPI: Age ≥60 (vs <60)	<b>1.54</b>	1.00-2.37	1.35	0.85-2.13	1.38	0.87-2.19	1.33	0.83-2.12
IPI: LDH >Upper limit (vs Normal)	<b>1.53</b>	1.01-2.31	1.14	0.74-1.77	1.15	0.73-1.81	1.29	0.82-2.05
<i>MYC</i> Rearranged (vs Wildtype)	1.62	0.88-3.00			1.71	0.89-3.27	1.86	0.93-3.69
<i>BCL2</i> Rearranged (vs Wildtype)	0.74	0.37-1.47			0.51	0.24-1.08	0.57	0.26-1.24
<i>BCL6</i> Rearranged (vs Wildtype)	1.21	0.71-2.04			0.94	0.53-1.65	1.00	0.55-1.83
EBV Status Positive (vs Negative)	1.54	0.86-2.78			1.29	0.67-2.47	1.65	0.82-3.30
<i>CD79B</i> Mutated (vs Wildtype)	1.43	0.81-2.53					0.76	0.38-1.49
<i>MYD88</i> Mutated (vs Wildtype)	<b>1.64</b>	1.08-2.48					<b>1.87</b>	1.10-3.20

**Cross-validated C-index**

**0.67**

**0.69**

**0.70**

*For the multivariable model, unknown was regarded as a separate category for these variables for which some data were missing (not reported).*

**Table 3B** – Prognostic impact of molecular aberrations and IPI risk factors on relapse/progression: univariable and multivariable analysis

	Cause-specific hazards (CSH) for relapse/progression							
	Univariable		Multivariable Model 1 IPI		Multivariable Model 2 (IPI + molecular aberrations WHO 2016)		Multivariable Model 3 (IPI + molecular aberrations WHO 2016 + MYD88 + CD79B)	
	HR	95%-CI	HR	95%-CI	HR	95%-CI	HR	95%-CI
IPI: >2 Extranodal Yes (vs No)	1.57	0.99-2.41	1.55	0.99-2.41	<b>1.63</b>	1.04-2.57	<b>1.81</b>	1.14-2.86
IPI: Stage III/IV (vs I/II)	<b>2.76</b>	1.63-4.68	<b>2.12</b>	1.22-3.67	<b>2.06</b>	1.17-3.63	<b>2.14</b>	1.19-3.82
IPI: ECOG Performance Score >2 (vs ≤1)	<b>4.48</b>	2.58-7.78	<b>4.48</b>	2.58-7.78	<b>5.09</b>	2.86-9.05	<b>4.60</b>	2.57-8.22
IPI: Age ≥60 (vs <60)	1.14	0.75-1.74	1.11	0.71-1.72	1.14	0.73-1.79	1.12	0.71-1.77
IPI: LDH >Upper limit (vs Normal)	0.98	0.64-1.50	0.77	0.49-1.21	0.77	0.48-1.22	0.82	0.51-1.31
<i>MYC</i> Rearranged (vs Wildtype)	1.63	0.86-3.09			1.84	0.94-3.49	1.90	0.96-3.77
<i>BCL2</i> Rearranged (vs Wildtype)	1.34	0.75-2.40			1.03	0.56-1.90	1.23	0.66-2.30
<i>BCL6</i> Rearranged (vs Wildtype)	1.01	0.57-1.78			0.89	0.49-1.59	0.91	0.49-1.68
EBV Status Positive (vs Negative)	0.79	0.36-1.71			0.66	0.29-1.49	0.79	0.34-1.86
<i>CD79B</i> Mutated (vs Wildtype)	<b>1.82</b>	1.06-3.13					1.23	0.64-2.36
<i>MYD88</i> Mutated (vs Wildtype)	<b>1.62</b>	1.06-2.48					1.42	0.85-2.37

**Cross-validated C-index**

**0.63**

**0.63**

**0.64**

For the multivariable model, unknown was regarded as a separate group (not reported).

**Table 4 – Mutated MYD88 improved the prognostic performance of the IPI.**

	Overall survival				Cause-specific hazard (CSH) for relapse/progression			
	Univariable		Multivariable		Univariable		Multivariable	
	HR	95%-CI	HR	95%-CI	HR	95%-CI	HR	95%-CI
<b>IPI-score</b> As continuous variable	1.73	1.45-2.08	1.77	1.47-2.13	1.45	1.21-1.73	1.47	1.22-1.76
<b>MYD88</b> Mutated (vs Wildtype)			1.83	1.19-2.80			1.69	1.09-2.60
<b>Cross-validated C-index</b>	<b>0.57</b>		<b>0.61</b>		<b>0.53</b>		<b>0.57</b>	



### **Figure legends**

#### **Figure 1 – Oncoprint plot of the molecular analysis of 250 cases with diffuse large B-cell lymphoma (DLBCL).**

Abbreviations: EBV – Epstein-Barr virus, GCB – germinal center B-cell, IP – immune-privileged. Of 52 cases, molecular analysis was not complete due to results that were not unambiguous to interpret or no FFPE material was left for subsequent analysis.

#### **Figure 2 – Molecular characterization discriminates distinct DLBCL subgroups with prognostic impact.**

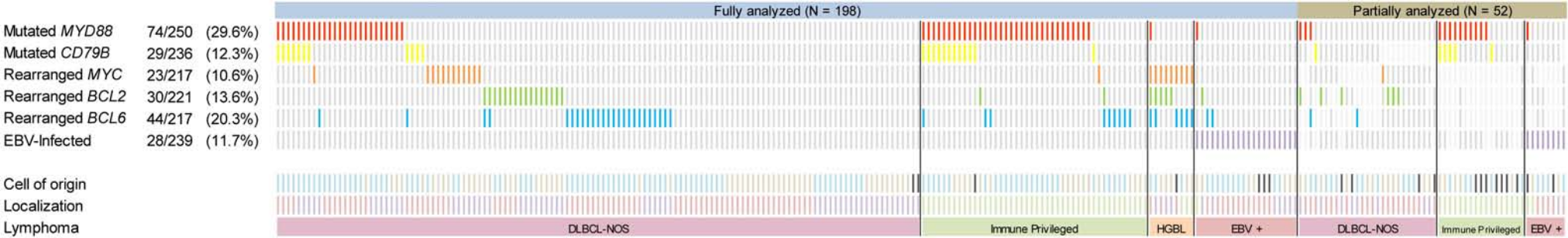
**(A)** Venn diagram demonstrating the overlap of aberrations for 198 fully analysed DLBCLs. **(B)** DLBCLs without detected aberrations showed a superior overall survival compared to DLBCLs with  $\geq 1$  affected aberrations (for cases with complete aberration analysis), identifying a novel good-risk group. **(C)** Progression free survival of the novel identified risk group (for cases with complete driver analysis). **(D)** Cumulative incidences of novel identified risk group (for cases with complete driver analysis).

Abbreviation: CRS – competing risk.

#### **Figure 3 – Prognostic significance of anatomical location, IPI Score and MYD88 in DLBCL.**

Overall survival (OS), progression free survival (PFS), and cumulative incidence of relapse/progression compared to non-relapse mortality (NRM) (1<sup>st</sup> row: Location, 2<sup>nd</sup> row: IPI Score, 3<sup>rd</sup> row: MYD88).

Abbreviation: CRS – competing risk.



= Abberations

= Non-GCB

= Mixed

= Infected

= GCB

= Immune Privileged

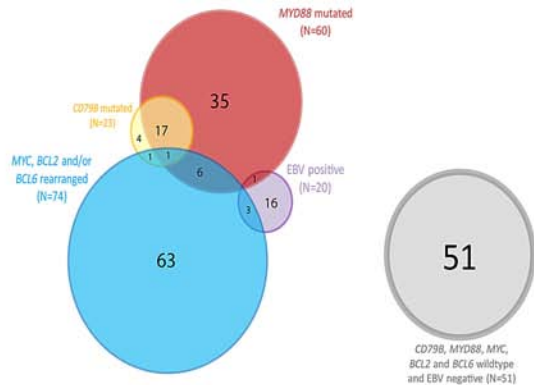
= Wildtype

= Unclassifiable

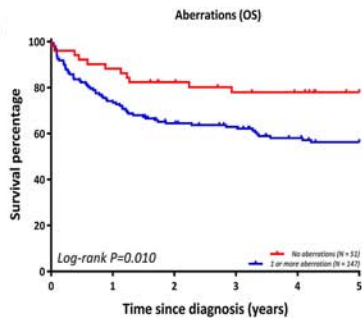
= Nodal

= Unknown

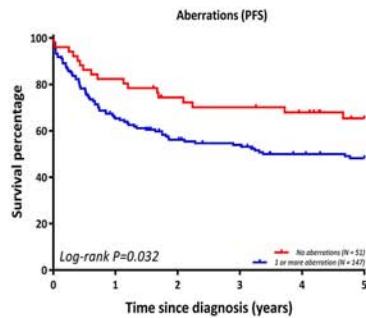
A



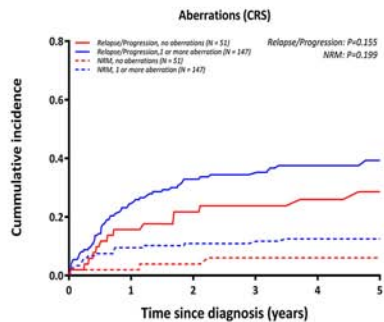
B



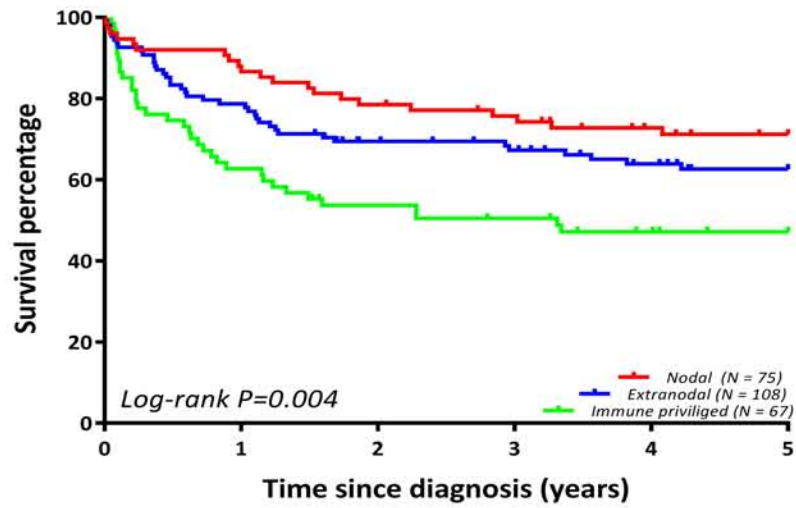
C



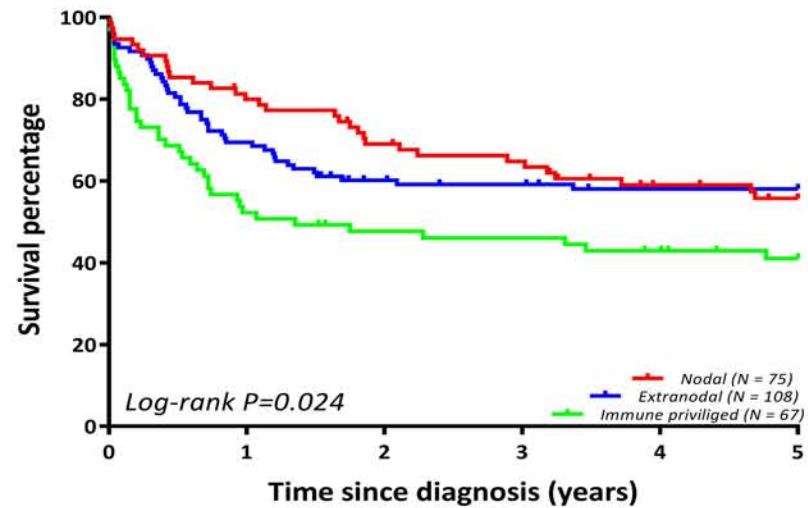
D



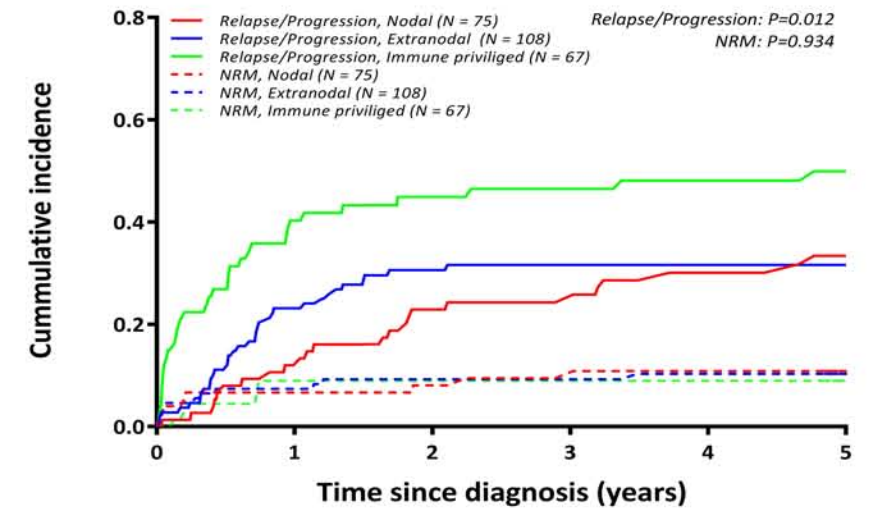
Localization (OS)



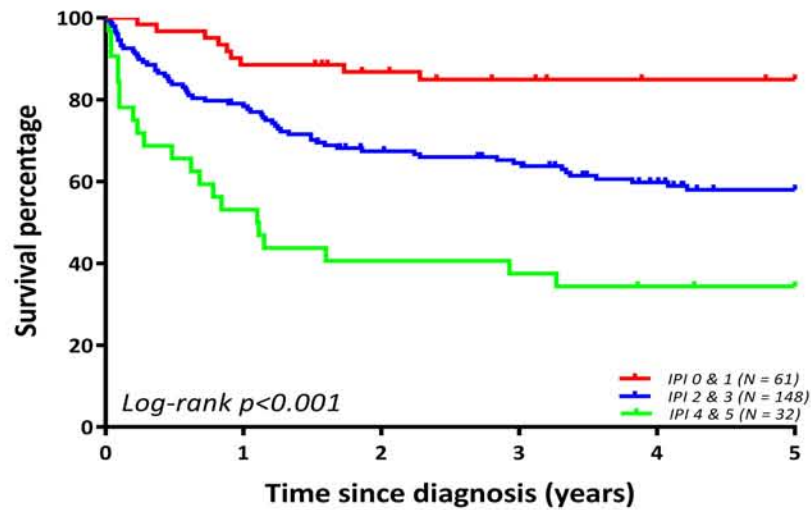
Localization (PFS)



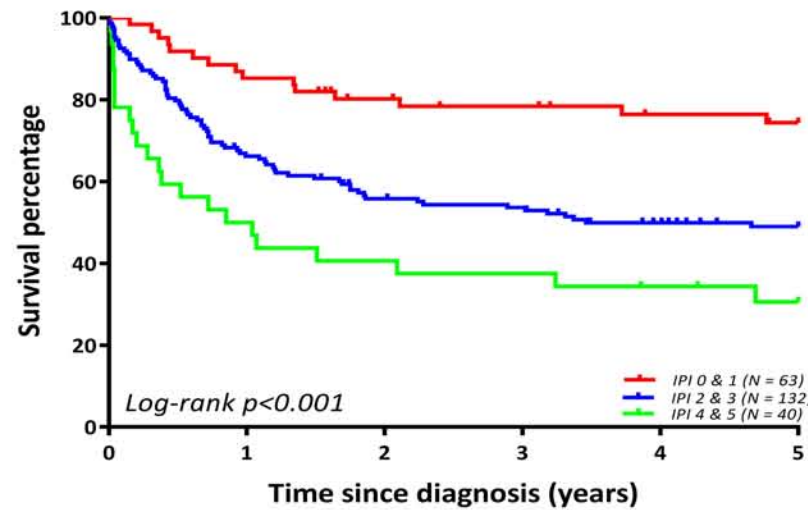
Localization (CRS)



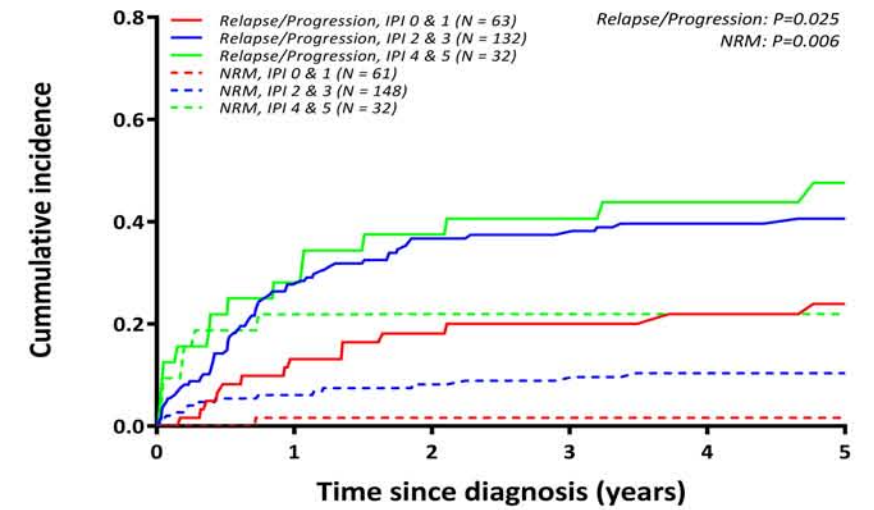
IPI Score (OS)



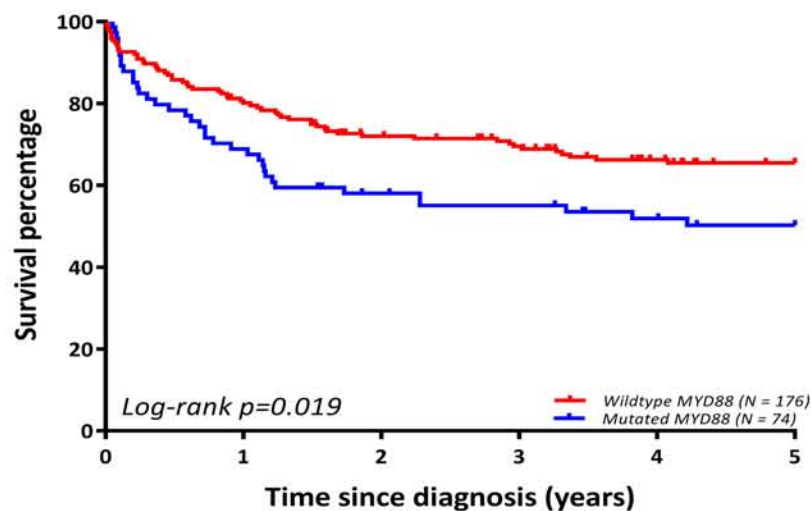
IPI Score (PFS)



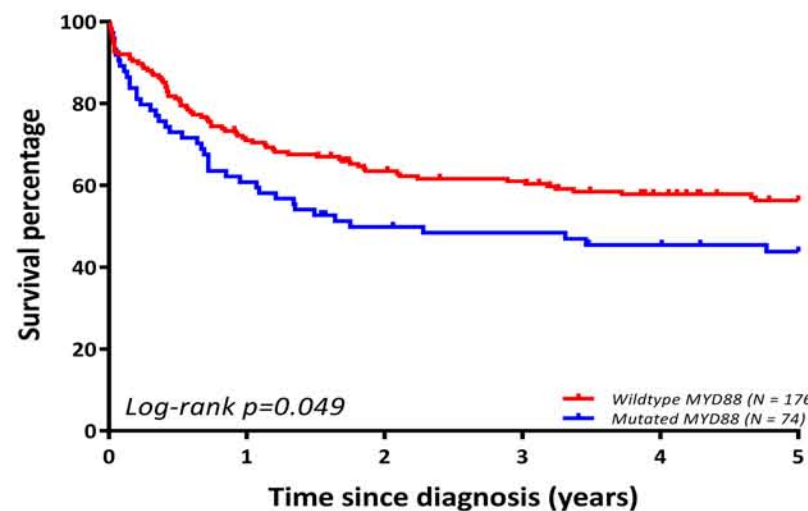
IPI Score (CRS)



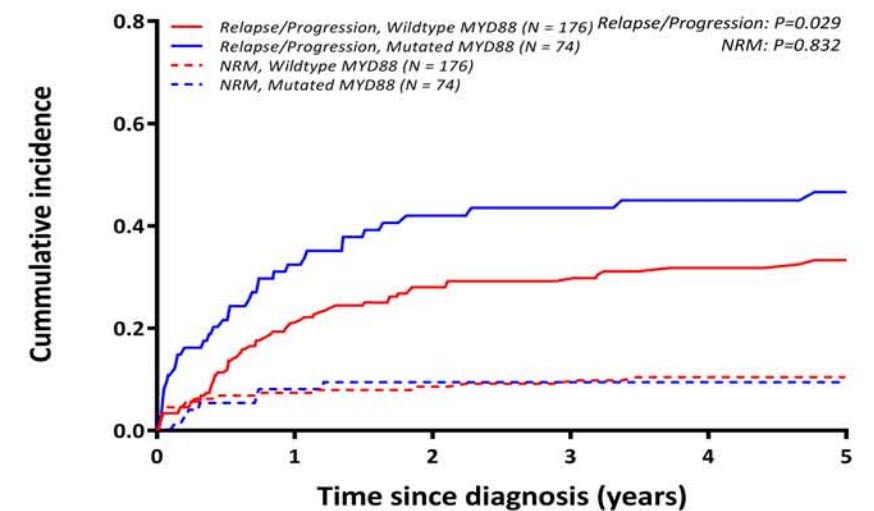
MYD88 (OS)



MYD88 (PFS)



MYD88 (CRS)



# MYD88 mutations identify a molecular subgroup of Diffuse Large B-Cell Lymphoma with an unfavourable prognosis

Joost S. Vermaat<sup>1,2,3</sup>, Sebastiaan F. Somers<sup>3</sup>, Liesbeth C. de Wreede<sup>4</sup>, Willem Kraan<sup>2,5</sup>, Ruben A.L. de Groen<sup>3</sup>, Anne M. R. Schrader<sup>6</sup>, Emile D. Kerver<sup>7</sup>, Cornelis G. Scheepstra<sup>8</sup>, Henriëtte Berenschot<sup>9</sup>, Wendy Deenik<sup>10</sup>, Jurgen Wegman<sup>1,11</sup>, Rianne Broers<sup>12</sup>, Jan-Paul D. de Boer<sup>13</sup>, Marcel Nijland<sup>14</sup>, Tom van Wezel<sup>6</sup>, Hendrik Veelken<sup>3</sup>, Marcel Spaargaren<sup>2,5</sup>, Arjen H. Cleven<sup>6</sup>, Marie José Kersten<sup>1,2</sup> and Steven T. Pals<sup>2,5</sup>

## Running heads:

MYD88 mutational status improves classification and prognostication in DLBCL

## Correspondence:

Joost S.P. Vermaat MD PhD MSc, Department of Hematology, Leiden University Medical Center, PO Box 9600, 2300 RC Leiden, The Netherlands  
E-mail: [j.s.p.vermaat@lumc.nl](mailto:j.s.p.vermaat@lumc.nl)

## Supplementary information

### Table of contents

#### *Supplemental methods.*

Antibodies for immunohistochemical staining, EBV and FISH

#### *Supplemental figure 1.*

Survival curves of Cell-of-Origin, MYC, BCL2 and BCL6 aberrations, EBV status, CD79B and High-grade B-cell lymphoma

#### *Supplemental table 1*

Prognostic impact of molecular aberrations, anatomical lymphoma location and IPI risk factors on overall survival: univariable and multivariable analysis

## Supplemental Methods - Antibodies for staining, EBV and FISH

### Immunohistochemical staining - antibodies:

The following immunohistochemical stains were performed with the DAKO Autostainer Link 48, Agilent (LUMC) or the Labvision Autostainer 480S from Thermo Fisher Scientific (AUMC), according to the manufacturer's recommendations, with the antibodies as listed in table 1.

Table 1. Antibodies:

	AUMC	LUMC
CD20	Clone L26, DAKO, Glostrup, Denmark	Clone L26, DAKO, Glostrup, Denmark
CD10	Clone 56C6, Thermo Fisher Scientific, Rockford, IL, USA	Clone 56C6, DAKO
MUM1	Clone MUM1p, DAKO, Glostrup, Denmark	Clone MUM1p, DAKO,
BCL2	Clone 124, DAKO, Glostrup, Denmark	Clone 124, DAKO Glostrup, Denmark
BCL6	Clone PG-B6p, DAKO, Glostrup, Denmark	Clone PG-B6p, Invitrogen

### Epstein-Barr virus early RNA *in situ* hybridization (EBER-ISH)

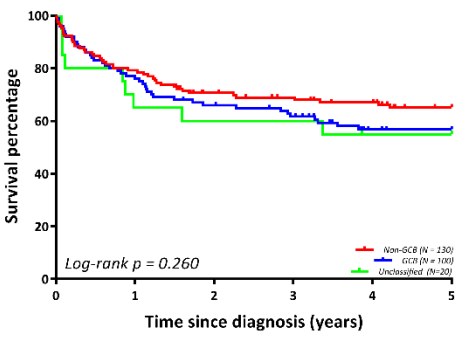
*In situ* hybridization for Epstein-Barr virus early RNA (EBER-ISH) was performed with EBER probes from Ventana (LUMC) or Biogenex (AUMC), according to the manufacturer's recommendations.

### Fluorescence *in situ* hybridization (FISH) for *MYC*, *BCL2* and *BCL6*

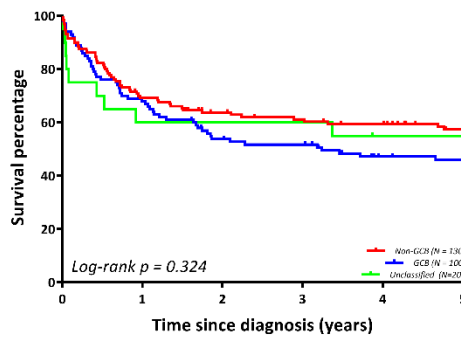
Fluorescence *in situ* hybridization was performed with break apart rearrangement probes for *MYC*, *BCL2* and *BCL6* from Abbott (LUMC) or DAKO (AUMC), with the DAKO Histology FISH Accessory Kit, Agilent, according to the manufacturer's recommendations.

# Supplemental figure 1 - Survival outcomes of COO and other aberrations

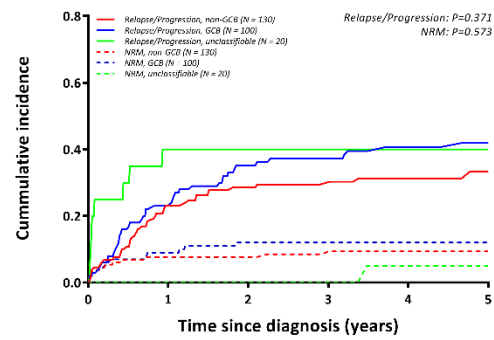
Supplemental 1A. Cell-of-Origin (OS)



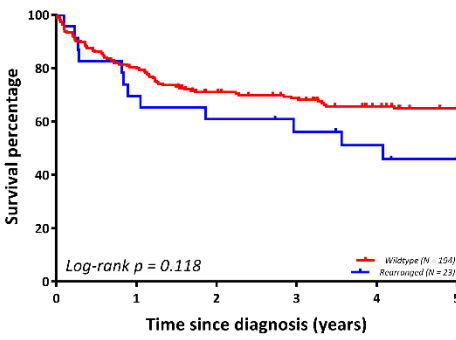
Supplemental 1B. Cell-of-Origin (PFS)



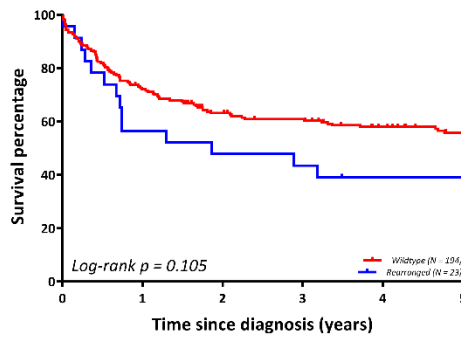
Supplemental 1C. Cell-of-Origin (CRS)



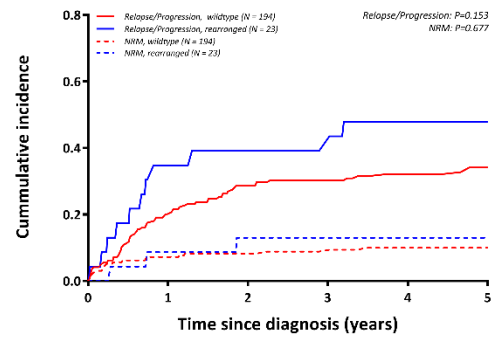
Supplemental 1D. MYC status (OS)



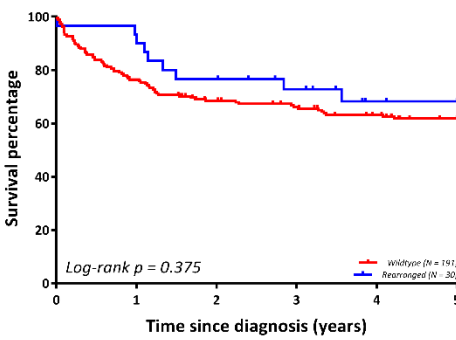
Supplemental 1E. MYC status (PFS)



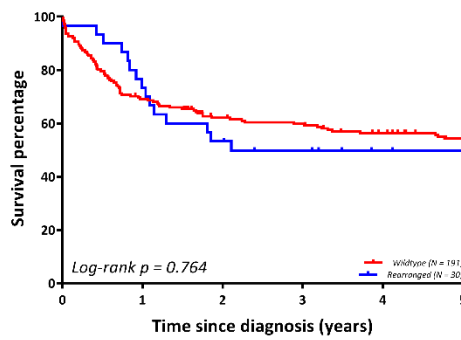
Supplemental 1F. MYC status (CRS)



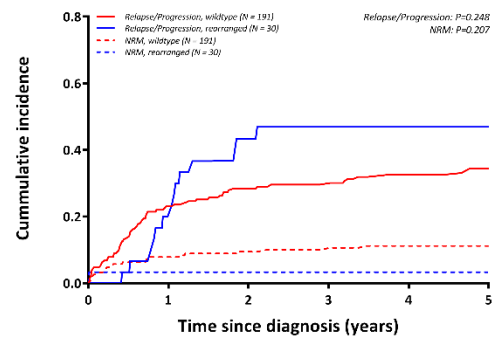
Supplemental 1G. BCL2 status (OS)



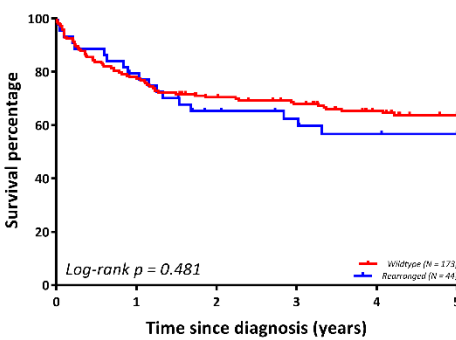
Supplemental 1H. BCL2 status (PFS)



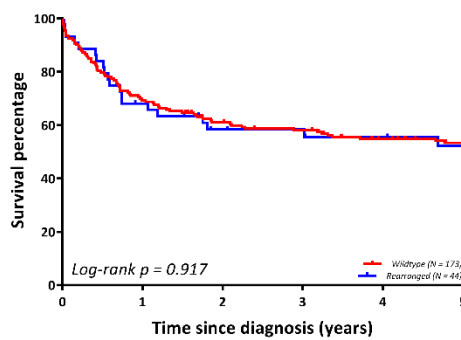
Supplemental 1I. BCL2 status (CRS)



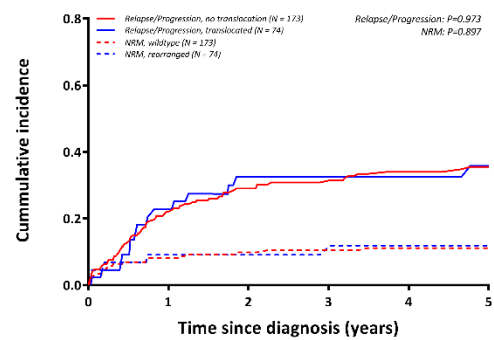
Supplemental 1J. BCL6 status (OS)



Supplemental 1K. BCL6 status (PFS)

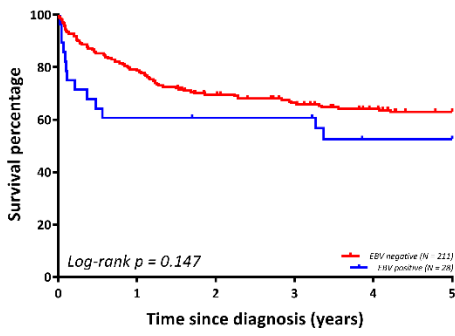


Supplemental 1L. BCL6 status (CRS)

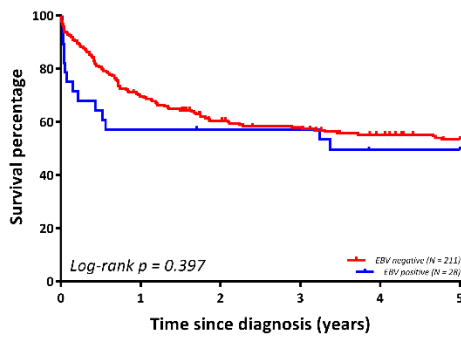


# Supplemental figure 1 - (continued)

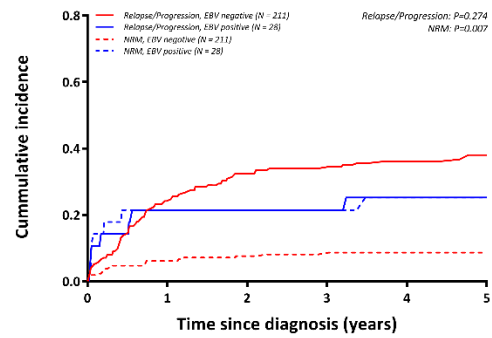
Supplemental 1M. EBV status (OS)



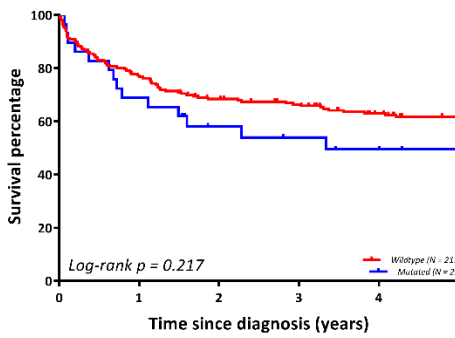
Supplemental 1N. EBV status (OS)



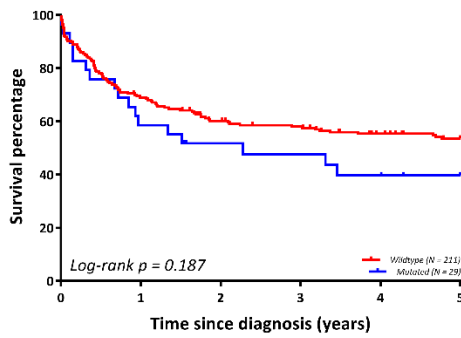
Supplemental 1O. EBV status (CRS)



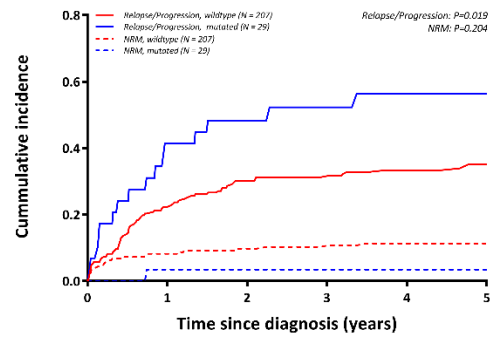
Supplemental 1P. CD79B status (OS)



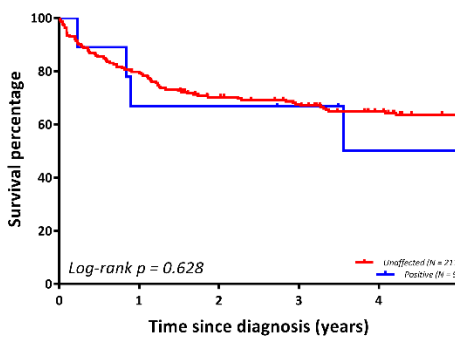
Supplemental 1Q. CD79B status (PFS)



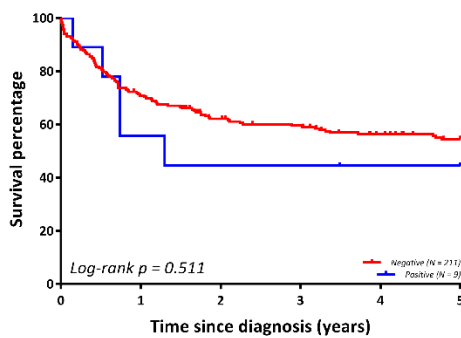
Supplemental 1R. CD79B status (CRS)



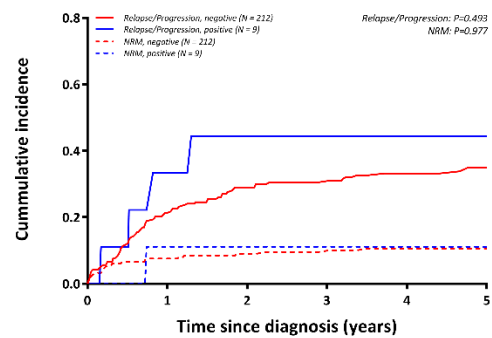
Supplemental 1S. High-grade B-cell lymphoma's (OS)



Supplemental 1T. High-grade B-cell lymphoma's (PFS)



Supplemental 1U. High-grade B-cell lymphoma's (CRS)





**Supplemental table 1 - Prognostic impact of molecular aberrations, anatomical lymphoma location and IPI risk factors on overall survival: univariable and multivariable analysis**

	Overall survival							
	Univariable		Multivariable Model 1 (IPI)		Multivariable Model 4 (IPI + anatomical localizations + aberrations WHO 2016)		Multivariable Model 5 (IPI + anatomical localizations + aberrations WHO 2016 + MYD88 + CD79B)	
	HR	95%-CI	HR	95%-CI	HR	95%-CI	HR	95%-CI
IPI: >2 Extranodal Yes (vs No)	1.37	0.91-2.07	1.41	0.90-2.22	1.59	0.92-2.74	1.64	0.96-2.80
IPI: Stage III/IV (vs I/II)	<b>2.33</b>	1.41-3.85	1.67	0.98-2.84	1.66	0.94-2.94	<b>1.87</b>	1.05-3.33
IPI: ECOG Performance Score >2 (vs ≤1)	<b>8.15</b>	5.23-12.7	<b>7.53</b>	4.67-12.15	<b>7.69</b>	4.65-12.72	<b>7.74</b>	4.64-12.92
IPI: Age ≥60 (vs <60)	<b>1.54</b>	1.00-2.37	1.35	0.85-2.13	1.25	0.78-2.00	1.24	0.77-2.00
IPI: LDH >Upper limit (vs Normal)	<b>1.53</b>	1.01-2.31	1.14	0.74-1.77	1.34	0.84-2.15	1.43	0.89-2.29
Anatomical localization Nodal								
Extranodal (+/- nodal)	1.42	0.83-2.41			1.39	0.74-2.62	1.55	0.81-2.93
Immune-privileged	<b>2.37</b>	1.38-4.08			<b>2.47</b>	1.30-4.71	<b>2.24</b>	1.08-4.62
<i>MYC</i> Rearranged (vs Wildtype)	1.62	0.88-3.00			<b>2.00</b>	1.03-3.91	1.92	0.95-3.85
<i>BCL2</i> Rearranged (vs Wildtype)	0.74	0.37-1.47			0.62	0.29-1.34	0.67	0.31-1.47
<i>BCL6</i> Rearranged (vs Wildtype)	1.21	0.71-2.04			0.96	0.54-1.71	0.92	0.50-1.70
EBV Status Positive (vs Negative)	1.54	0.86-2.78			1.65	0.84-3.23	1.72	0.86-3.45
<i>CD79B</i> Mutated (vs Wildtype)	1.43	0.81-2.53					0.68	0.34-1.35
<i>MYD88</i> Mutated (vs Wildtype)	<b>1.64</b>	1.08-2.48					1.45	0.78-2.71

**Cross-validated C-index**

**0.67**

**0.71**

**0.71**

*For the multivariable model, unknown was regarded as a separate category for these variables for which some data were missing (not reported)*

